ELSEVIER

Comput. Methods Appl. Mech. Engrg. 190 (2001) 5907–5922

Computer methods in applied mechanics and engineering

www.elsevier.com/locate/cma

A point interpolation method for simulating dissipation process of consolidation

J.G. Wang *, G.R. Liu, Y.G. Wu

Department of Mechanical and Production Engineering, Centre of Advanced Computations in Engineering Science, National University of Singapore, 10 Kent Ridge Crescent, Singapore 119260, Singapore

Received 20 October 1999; received in revised form 9 October 2000

Abstract

A Biot's consolidation problem in foundation engineering is numerically investigated using improved point interpolation method (PIM). A weak form of Biot's theory is first developed to consider the unbalanced forces at previous time-step and thus guarantees the global equilibrium at current step. Two independent variables in the weak form, displacement and excess pore water pressure, are approximated using the same shape functions through PIM technique. The PIM technique constructs its interpolation functions through a cluster of scattered points in problem domain and its shape function is of delta properties, thus implementation of essential boundary conditions is as easy as in conventional finite element method. Crank–Nicholson's integration scheme is used to discretize time domain. Finally, examples are studied and compared with finite element methods to demonstrate its capability.

Keywords: Meshless method; Polynomial interpolation; Coordinates transformation; Consolidation process; Pore water pressure

1. Introduction

Finite element method (FEM) has now made numerical simulation a daily activity in engineering science. However, difficulties are encountered when mesh distortion is dealt with FEM. Mesh distortion may be induced by large deformation, crack growth and movement of free surface. This is due to the essential properties of element-based shape function. One solution for such a problem is to remesh the problem domain and to use adaptive algorithm in computation. This remeshing process is time consuming and sometimes causes mesh-size dependent results (for example the crack tip problem of creep). One effective numerical method is meshless method that does not require any element for shape function.

Some element-free or meshless methods were proposed and have achieved remarkable progress in recent years. For example, diffuse element method (DEM) [1] used a cluster of scattered nodes instead of elements to construct shape functions through moving least-square method (MLS). Reproducing kernel particle method (RKPM) [2] was proposed through a correction function and a window function. Hp-cloud method [3] was proposed to simulate particle interaction through the partition of unit method. A finite point method (FPM) was proposed to solve fluid mechanics problem by Onate et al. [4] through only nodal integral. Belytschko and his colleagues [5–7] proposed a meshless method called element-free Galerkin (EFG) method. This method uses MLS to construct its shape function and Galerkin procedure to establish its system equation. EFG method has been applied to a large variety of problems such as solid problems, deformable multiphase porous media [8].

* Corresponding author.

0045-7825/01/$ - see front matter
PII: S0045-7825(01)00204-3

The original MLS is proposed for surface fitting over scattered data points by Lancaster and Salkauskas [9]. It does not require its approximation pass through data points or its shape function lacks of delta function properties. Thus, following major technical disadvantages always accompany with the meshless methods based on MLS approximation: (1) Difficulties in the implementation of essential boundary conditions; (2) complexity of algorithms to construct shape functions. For the first problem, many methods are proposed to treat essential boundary condition such as Lagrangian method [5], penalty method [10], collocation method [11] and other method [12]. For the second problem, useful suggestions are proposed such as analytical integration [2], recursive method [13] and parallel computing [14]. All of these efforts can improve computation efficiency. A new interpolation scheme called point interpolation method (PIM) was proposed to solve above two problems [15,16] from the view of point interpolation. The PIM method has its shape function with delta properties and only once inverse matrix is required for its function and derivatives. Thus it is of high computation efficiency.

This paper discusses the numerical solution of Biot's consolidation theory in foundation engineering using the PIM method. First, a general form of Biot's consolidation theory is stated. This form of Biot's consolidation problems can accommodate any constitutive law of materials. Then, the weak form is obtained by imposition of global equilibrium at each time-step and thus an unequilibrium potential principle is developed. Spatial variables, displacement and pore pressure, are discretized in the same PIM interpolation schemes. Crank–Nicholson method is used for the discretization of time domain. Finally, one- and two-dimensional examples are calculated and compared with closed-form solution or FEM results.

2. Biot's consolidation theory and its weak form

For saturated soil, soil skeleton and water consist of soil–water mixture. These two systems interact at micro-level. Biot's consolidation theory [17] provides a macro-level description for the interactions. It is composed of following six concepts:

- Equilibrium equation of soil–water mixture

$$\frac{\partial \sigma_{ij}}{\partial x_j} + b_i = 0 \quad \text{in } V \tag{1}$$

or its incremental form in time interval $[t, t+\Delta t]$

$$\frac{\partial \Delta\sigma_{ij}}{\partial x_j} + \Delta b_i = -\left(\frac{\partial \sigma^t_{ij}}{\partial x_j} + b^t_i\right) \quad \text{in } V. \tag{2}$$

- Relationship of displacement and strain for soil skeleton

$$\Delta\varepsilon_{ij} = \frac{1}{2}\left(\frac{\partial \Delta u_i}{\partial x_j} + \frac{\partial \Delta u_j}{\partial x_i}\right) \quad \text{in } V. \tag{3}$$

- Constitutive law of soil skeleton in differential form

$$\mathrm{d}\sigma'_{ij} = D^{\mathrm{ep}}_{ijkl}\,\mathrm{d}\varepsilon_{kl} \quad \text{in } V. \tag{4}$$

- Darcy's seepage law for pore water flow

$$q_i = \frac{K_{ij}}{\gamma_{\mathrm{w}}}\frac{\partial u}{\partial x_j} \quad \text{in } V. \tag{5}$$

- Terzaghi's effective stress principle

$$\sigma_{ij} = \sigma'_{ij} + u\delta_{ij}. \tag{6}$$

- Incompressibility of solid–water mixture or continuity equation

$$\frac{\partial \varepsilon_{\mathrm{v}}}{\partial t} = \frac{\partial q_i}{\partial x_i}, \tag{7}$$

where σ_{ij}, σ'_{ij} and u are total stress tensor, effective stress tensor and excess pore water pressure at any time t and b_i is the unit body force. Δu_i is the displacement increment and $\Delta\sigma_{ij}$, $\Delta\varepsilon_{ij}$ total stress and strain increments in time interval $[t, t+\Delta t]$. The discharge of excess pore water is q_i in ith direction. γ_w is the density of water. In SI system, its value can be taken as 10 kN/m^3. D^{ep}_{ijkl} is the elastoplastic matrix of soil skeleton which is determined by constitutive laws. K_{ij} is permeability tensor of soil skeleton which usually has non-zero components K_x in x-direction and K_y in y-direction, respectively. ε_{v} is the volume strain of soil skeleton which is expressed as

$$\varepsilon_{\mathrm{v}} = \frac{\partial u_i}{\partial x_i}. \tag{8}$$

Boundary conditions for this problem include two parts: boundary for solid and boundary for fluid

For soil skeleton boundary

$$\begin{cases} u_i = \bar{u}_{i0} \\ \sigma'_{ij} n_j = \bar{T}_i \end{cases} \quad \text{on } S_{\bar{u}} \times [0,\infty), \tag{9}$$

where $\mathbf{n} = \{n_1\ n_2\ n_3\}$ is the outwards normal direction and n_i is its directional cosine.

For fluid boundary

$$\begin{cases} u = u_0 \\ q_i = q_{i0} \end{cases} \quad \text{on } S_u \times [0,\infty). \tag{10}$$

Initial condition

$$\begin{cases} u_i = 0 \\ u = 0 \end{cases} \quad \text{on } V \times 0^-. \tag{11}$$

Two components of body forces are acting on the soil skeleton:

1. Effective unit weight b'_i $(= b_i - \gamma_{\mathrm{w}})$.
2. Seepage force induced by hydraulic gradient $(-(\partial u/\partial x_i))$.

If a time interval $[t, t+\Delta t]$ is considered, increments of soil skeleton during this time interval should satisfy the weak form of equilibrium equation (2) of soil skeleton

$$\begin{aligned} &\int_v \{\delta(\Delta\varepsilon)\}^{\mathrm{T}}\{\Delta\sigma'\}\,\mathrm{d}v - \int_v \left\{\delta\left(\frac{\partial \Delta u_i}{\partial x_i}\right)\right\}^{\mathrm{T}}\{u\}^{t+\Delta t}\,\mathrm{d}v - \int_v \left\{\delta(\Delta\bar{u})\right\}^{\mathrm{T}}\{\Delta b\}\,\mathrm{d}v \\ &\quad + \int_{S_\sigma} \left\{\delta(\Delta\bar{u})\right\}^{\mathrm{T}}\{n\}u^{t+\Delta t}\,\mathrm{d}s - \int_{S_\sigma} \left\{\delta(\bar{u})\right\}^{\mathrm{T}}\left\{\Delta\bar{T}\right\}\mathrm{d}s \\ &\quad = -\int_v \{\delta(\Delta\varepsilon)\}^{\mathrm{T}}\{\sigma''\}\,\mathrm{d}v + \int_{S_\sigma} \left\{\delta(\bar{u})\right\}^{\mathrm{T}}\left\{\bar{T}\right\}^{t}\mathrm{d}v - \int_v \left\{\delta(\Delta\bar{u})\right\}^{\mathrm{T}}\{b^t\}\,\mathrm{d}v. \end{aligned} \tag{12}$$

The term at the right-hand side includes the unbalanced force at previous time-step. This force can be automatically corrected and thus Eq. (12) can prevent error accumulation at each step and keep global balance at any time. Thus the same accuracy is achieved at each time step. This auto-corrector is specially useful in incremental computation schemes for dissipation or nonlinear problems.

Time integration is applied to continuity equation (8) and then the weak form for spatial variables (x, y) is expressed as

$$-\int_v \{\delta u\}^{\mathrm{T}}\left\{\frac{\partial \Delta u_i}{\partial x_i}\right\}\mathrm{d}v = \frac{1}{\gamma_{\mathrm{w}}}\int_t^{t+\Delta t}\left[\int_{S_q}\{\delta u\}^{\mathrm{T}}\{Ku\}\,\mathrm{d}s\right]\mathrm{d}t + \frac{1}{\gamma_{\mathrm{w}}}\int_t^{t+\Delta t}\left[\int_v \left\{\frac{\partial \delta u}{\partial x_i}\right\}^{\mathrm{T}}\left\{K_i\frac{\partial u}{\partial x_i}\right\}\mathrm{d}v\right]\mathrm{d}t, \tag{13}$$

where δu expresses the variational of displacement and excess pore water pressure.

3. PIM interpolation and its shape functions

PIM interpolates a cluster of scattered data points to construct its shape functions for displacement increments and excess pore water pressure. If a set of arbitrarily distributed points $P_i(x_i)$ $(i = 1, 2, \ldots, n)$ and their function values u_i (displacement and pore water pressure) are given surrounding point x, the PIM method constructs a continuous surface $u(x)$ using polynomial basis functions as

$$u(x) = \sum_{i=1}^{n} p_i(x) a_i(x) = \mathbf{p}^{\mathrm{T}}(x)\mathbf{a}, \tag{14}$$

where $p_i(x)$ is monomials in co-ordinates $\mathbf{x}^{\mathrm{T}} = [x, y]$ for two-dimensional problems. n is the number of nodes in the neighborhood of x (this neighborhood is called influence domain of x), a_i is the coefficient of $p_i(x)$ and

$$\mathbf{a}^{\mathrm{T}} = [\, a_1 \quad a_2 \quad \cdots \quad a_n \,]. \tag{15}$$

The coefficients a_i are determined by letting the function $u(x)$ in Eq. (14) pass through all n-scattered points. Interpolation at the ith point is expressed as

$$u_i = \mathbf{P}^{\mathrm{T}}(x_i)\mathbf{a}, \quad i = 1, 2, \ldots, n. \tag{16}$$

It is noted that u_i is the nodal value of u at $x = x_i$, while MLS just gives a displacement index. Rewriting of Eq. (16) gets an equation set on unknowns $\mathbf{a}$

$$\mathbf{u}^{\mathrm{e}} = \mathbf{P}_0\mathbf{a}, \tag{17}$$

where

$$\begin{aligned} \mathbf{u}^{\mathrm{e}} &= [\, u_1 \quad u_2 \quad u_3 \quad \cdots \quad u_n \,]^{\mathrm{T}}, \\ \mathbf{P}_0 &= [\, \mathbf{p}(x_1) \quad \mathbf{p}(x_2) \quad \cdots \quad \mathbf{p}(x_n) \,]^{\mathrm{T}}. \end{aligned} \tag{18}$$

If the inverse of matrix $\mathbf{P}_0$ exists, a unique solution on $\mathbf{a}$ is obtained as

$$\mathbf{a} = \mathbf{P}_0^{-1}\mathbf{u}^{\mathrm{e}} \tag{19}$$

and the interpolation function is expressed as

$$u(x) = \boldsymbol{\varphi}(x)\mathbf{u}^{\mathrm{e}}, \tag{20}$$

where the shape function $\boldsymbol{\varphi}(x)$ is defined as

$$\boldsymbol{\varphi}(x) = \mathbf{P}^{\mathrm{T}}(x)\mathbf{P}_0^{-1} = [\, \phi_1(x) \quad \phi_2(x) \quad \cdots \quad \phi_n(x) \,]. \tag{21}$$

Shape function $\phi_i(x)$ depends only on the distribution of scattered nodes. It has the following properties:

1. $\phi_i(x)$ has the same basis as $\mathbf{p}(x)$ in local influence domain.
2. $\phi_i(x)$ is a polynomial and its order is the same as basis functions $\mathbf{p}(x)$.
3. $\phi_i(x)$ is of delta function properties expressed as follows

$$\phi_i(x) = \begin{cases} 1, & x = x_i, \\ 0, & x = x_j \quad (j \neq i). \end{cases} \tag{22}$$

4. $\phi_i(x)$ is of unity partition properties as

$$\sum_{i=1}^{n} \phi_i(x) = 1. \tag{23}$$

It should be noted that there does not require $0 \leqslant \phi_i(x) \leqslant 1$.

The key for the PIM method with polynomial basis function is how to guarantee the existence of shape functions or P_0^{-1} . The no-existence or instability is from rank deficiency of basis functions. Some numerical

techniques are helpful to alleviate this problem. For example, following rules are useful when a basis function is constructed: (1) Bivariate method (see [18]) is applicable if the measure of scattered nodes is suitable. (2) Basis is as complete as possible if nodes number is the same. (3) Any cluster of scattered nodes should have at least one set of linearly independent basis.

In order to avoid the singularity of matrix $\mathbf{P}_0$, Liu and Gu [15] proposed a moving node method to slightly change the coordinates of nodes. Changing basis function is an effective method [16]. This change can be carried out through a local coordinate transformation. That is, global coordinates (x, y) are firstly translated to the Gauss point (x_0, y_0) where function is to be interpolated, then rotation with an angle θ is applied if necessary. This coordinates transformation is expressed as

$$\begin{aligned} \zeta &= (x - x_0)\cos\theta + (y - y_0)\sin\theta, \\ \eta &= -(x - x_0)\sin\theta + (y - y_0)\cos\theta \end{aligned} \tag{24}$$

or its inverse is expressed as

$$\begin{aligned} x &= x_0 + (\zeta\cos\theta - \eta\sin\theta), \\ y &= y_0 + (\zeta\sin\theta + \eta\cos\theta), \end{aligned} \tag{25}$$

where (ζ, η) are the local or new coordinates. $p_i(\zeta)$ is determined from this local coordinates and thus the $\mathbf{P}_0^{-1}$ is the inverse under local coordinates instead of global coordinates. Derivatives at Gauss point are simple if the basis functions are monomials. In local coordinates, the derivatives are expressed as:

$$\begin{aligned} \left.\frac{\partial\phi}{\partial\zeta}\right|_{(0,0)} &= (0, 1, 0, \ldots, 0)P_0^{-1}, \\ \left.\frac{\partial\phi}{\partial\eta}\right|_{(0,0)} &= (0, 0, 1, 0, \ldots, 0)P_0^{-1}. \end{aligned} \tag{26}$$

The derivatives in global coordinates are obtained through coordinate rotations:

$$\begin{Bmatrix} \dfrac{\partial\phi}{\partial x} \\ \dfrac{\partial\phi}{\partial y} \end{Bmatrix} = \begin{bmatrix} \cos\theta & -\sin\theta \\ \sin\theta & \cos\theta \end{bmatrix} \begin{Bmatrix} \left.\dfrac{\partial\phi}{\partial\zeta}\right|_{(0,0)} \\ \left.\dfrac{\partial\phi}{\partial\eta}\right|_{(0,0)} \end{Bmatrix}. \tag{27}$$

After this transformation, basis functions in global coordinates have the same order for x and y.

4. Discretization of weak form

Displacement increment $(\Delta u, \Delta v)$ and excess pore water pressure u at any time t is discretized by the interpolation given by Eq. (20). That is, at any point interpolations are expressed as

$$\begin{Bmatrix} \Delta u \\ \Delta v \\ u \end{Bmatrix} = \begin{bmatrix} \phi_1 & 0 & 0 & \cdots & \phi_n & 0 & 0 \\ 0 & \phi_1 & 0 & \cdots & 0 & \phi_n & 0 \\ 0 & 0 & \phi_1 & \cdots & 0 & 0 & \phi_n \end{bmatrix} \mathbf{u}^{\mathrm{T}}, \tag{28}$$

where the nodal vector $\mathbf{u}$ is

$$\mathbf{u} = [\,\Delta u_1 \quad \Delta v_1 \quad u_1 \quad \Delta u_2 \quad \Delta v_2 \quad u_2 \quad \ldots \quad \Delta u_n \quad \Delta v_n \quad u_n\,]. \tag{29}$$

Time domain is integrated by the following equation for any function $f(x)$:

$$\int_t^{t+\Delta t} f(x)\,\mathrm{d}x = \Delta t[\theta f(t) + (1 - \theta)f(t + \Delta t)]. \tag{30}$$

Here $0 \leqslant \theta \leqslant 1$. After discretization of Eqs. (12) and (13), the following system equation is obtained:

$$\mathbf{Ku} = \mathbf{f}, \tag{31}$$

where

$$\begin{aligned} K_{ij} &= \int_v [K_{ij}^0]\,\mathrm{d}v = \sum_{k=1}^{N_{\text{gauss}}} K_{ij}^0 w_k \\ f_i &= \int_{S_\sigma} \phi_i \bar{\mathbf{t}}\,\mathrm{d}\Gamma + \int_v \phi_i \mathbf{b}\,\mathrm{d}v + \int_v f_{oi}\,\mathrm{d}v. \end{aligned} \tag{32}$$

System stiffness matrix is the summation over all Gaussian points (N_{gauss} refers to the Gauss number and w_k is the weight at the kth Gauss point). The stiffness at each Gauss point is composed of three parts: deformation of soil skeleton, pore water flow and their interaction. A typical expression of stiffness matrix for general constitutive laws is as

$$\left[K_{ij}^0\right] = \begin{bmatrix} P_1 d_1 + P_3 d_2 + P_3 d_3 + P_9 d_4 & P_3 d_1 + P_9 d_2 + P_2 d_3 + P_5 d_4 & -\phi_j \frac{\partial \phi_i}{\partial x} \\ P_3 d_1 + P_2 d_2 + P_9 d_3 + P_5 d_4 & P_9 d_1 + P_5 d_2 + P_5 d_3 + P_4 d_4 & -\phi_j \frac{\partial \phi_i}{\partial y} \\ -\phi_i \frac{\partial \phi_j}{\partial x} & -\phi_i \frac{\partial \phi_j}{\partial y} & K_{33}^0 \end{bmatrix}. \tag{33}$$

Four forces contribute load vectors: external load (T_i) , effective body force (b_i'), seepage force from pore water and unbalanced force at previous time-step. The forces f_{0i}, which are related to previous time-step, can be obtained through the following conversion:

$$\begin{Bmatrix} f_{0x} \\ f_{0y} \\ f_{0u} \end{Bmatrix} = \begin{Bmatrix} \frac{\partial \phi_i}{\partial x} \sigma_x' + \frac{\partial \phi_i}{\partial y} \tau_{xy} \\ \frac{\partial \phi_i}{\partial y} \sigma_y' + \frac{\partial \phi_i}{\partial x} \tau_{xy} \\ \theta \frac{\Delta t}{\gamma_w} \left[K_x \frac{\partial \phi_i}{\partial x} \sum_r \frac{\partial \phi_r}{\partial x} u_r^t + K_y \frac{\partial \phi_i}{\partial y} \sum_r \frac{\partial \phi_r}{\partial y} u_r^t \right] \end{Bmatrix}. \tag{34}$$

Material matrix $\mathbf{D}$ (its component is D_{ijkl}^{ep}) in Eq. (4) is generally expressed as follows:

$$\mathbf{D} = \begin{bmatrix} P_1 & P_2 & P_3 \\ P_2 & P_4 & P_5 \\ P_3 & P_5 & P_9 \end{bmatrix} \quad \text{for plane problem.} \tag{35}$$

For linear elasticity with Young's modulus, E, and Poisson ratio, v, the matrix is

$$\mathbf{D} = \frac{E}{1 - v^2} \begin{bmatrix} 1 & v & 0 \\ v & 1 & 0 \\ 0 & 0 & (1 - v)/2 \end{bmatrix} \quad \text{for plane stress.} \tag{36}$$

Other coefficients are denoted as

$$\begin{aligned} d_1 &= \frac{\partial \phi_i}{\partial x} \frac{\partial \phi_j}{\partial x}, \quad d_2 = \frac{\partial \phi_i}{\partial y} \frac{\partial \phi_j}{\partial x}, \\ d_3 &= \frac{\partial \phi_i}{\partial x} \frac{\partial \phi_j}{\partial y}, \quad d_4 = \frac{\partial \phi_i}{\partial y} \frac{\partial \phi_j}{\partial y}, \\ K_{33}^0 &= -(1 - \theta) \frac{\Delta t}{\gamma_w} \left(K_x d_1 + K_y d_4 \right). \end{aligned} \tag{37}$$

Flowchart for numerical algorithm is briefly given as follows:

1. Determine all Gauss points (position and weight) over background mesh.
2. Remove the background mesh.
3. Loop over Gauss points to assemble stiffness and load vector
   (a) Determine domain of influence for specified Gauss point and select neighboring nodes based on a defined criterion.

(b) Compute shape function and its derivatives for each Gauss point.
(c) Evaluate stiffness and loading at each Gauss point.
(d) Assemble contribution to form nodal system equation.
4. Solve system equation to obtain displacement increment and excess pore water pressure at each node.
5. Evaluate strain and effective stress at each Gauss point.
6. Preparation for next time-step.

5. Numerical examples

5.1. One-dimensional consolidation problem

As an example, a two-dimensional program studies one-dimensional consolidation problem. The two-dimensional program is designed for plane strain problems. The PIM model (regular node distribution) is shown in Fig. 1. Only upper surface is permeable and the rest impervious. Two sides and bottom are all fixed for displacements. Therefore, this is a single-side drainage problem. Thickness of soil layer is assumed to be $H = 16$ m. Soil parameters are regarded as linear elasticity with $E = 40\,000$ kPa and $v = 0.3$. When a surcharge $\Delta\sigma = 10$ kPa is suddenly applied on the surface of soil layer, excess pore water pressure will be generated by the program through a short-time increment. The excess pore water pressure thereafter dissipates with time.

This problem has a closed-form solution (see [19]) for excess pore water pressure:

$$u = \frac{4}{\pi}\Delta\sigma \sum_{n=1}^{\infty} \frac{1}{2n-1} \sin\left(\frac{(2n-1)\pi y}{2H}\right) \exp\left\{-(2n-1)^2 \frac{\pi^2}{4} T_v\right\}. \tag{38}$$

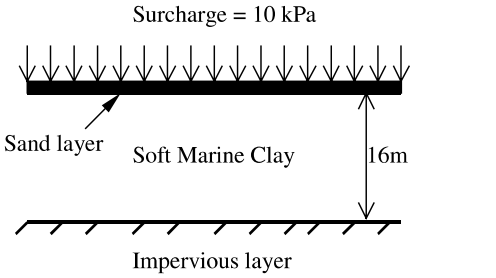

(a)

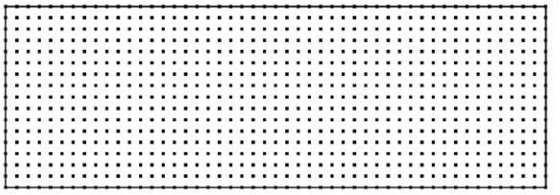

(b)

Sample point	Coordinates	Remarks
3	(24, 3)	Three points in one vertical line
10	(24, 10)	
14	(24, 14)	

(c)

Fig. 1. One-dimensional Terzaghi's consolidation problem: (a) one-dimensional consolidation problem; (b) nodal distribution for PIM method; (c) positions for the three sample points.

Degree of consolidation U_t is

$$U_t = 1 - \frac{8}{\pi^2}\sum_{n=1}^{\infty}\frac{1}{(2n-1)^2}\exp\left\{-(2n-1)^2\frac{\pi^2}{4}T_v\right\}, \tag{39}$$

where the parameters are defined as

$$T_v = \frac{C_v}{H^2}t, \quad C_v = \frac{k}{\gamma_w m_v}, \quad m_v = \frac{(1+v)(1-2v)}{E(1-v)}. \tag{40}$$

Surface settlement S_t at any time t is given by

$$S_t = U_t m_v \Delta\sigma H. \tag{41}$$

$\theta = 0.5$ is taken in numerical computation, which corresponds to Crank–Nicholson method. Time-step is automatically selected to keep stability and oscillation-free.

$$\frac{h^2}{6C_v} \leqslant \Delta t \leqslant \frac{h^2}{2C_v}, \tag{42}$$

where h is the characteristic size of node distance. For example, for the one-dimensional model, the h is the distance between two neighboring nodes.

Case 1 (*Constant permeability along depth*). The permeability is $k = 1.728 \times 10^{-3}$ m/day (or 2×10^{-8} m/s) in all directions. This is a standard Terzaghi problem and closed-form solution was already given. Surface settlement is given in Fig. 2 and history of excess pore water pressure is given in Fig. 3 for three sample points. Fig. 4 gives the spatial distribution of excess pore water pressure at different time. They are all in good agreement with closed-form solution.

Case 2 (*Variable permeability along depth*). Marine clay is soft clay and its permeability will vary with depth. A linear variable permeability with depth will be studied here. The permeability at the top surface is assumed to be 100 times the permeability at the bottom ($k = 1.728 \times 10^{-3}$ m/day). The permeability in between is assumed to be linear. For comparison, averaged permeability at top and bottom is used to get closed-form solution, which is used only for reference. Magnitude comparison is made through FEM with four nodal isoparameteric element. Fig. 5 shows the history of excess pore water pressure. Closed-form solution and FEM result are also plotted for comparison. The PIM and FEM results agree very well while

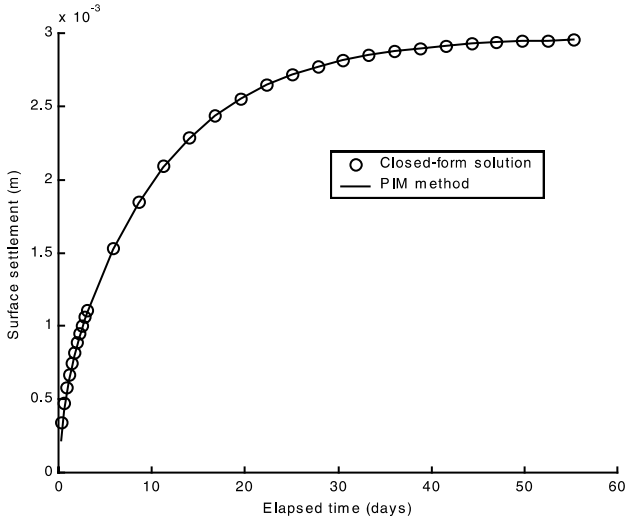

Fig. 2. Surface settlement with time.

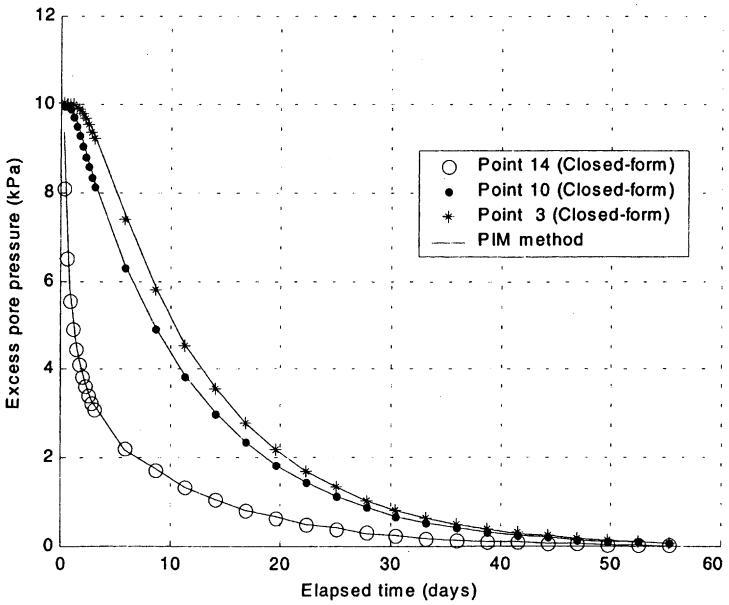

Fig. 3. Dissipation of excess pore water pressure at different points.

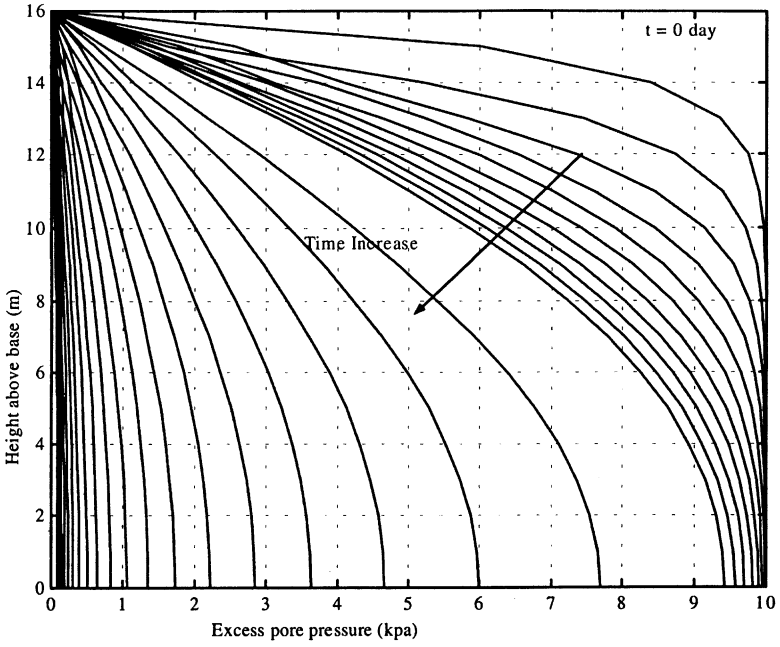

Fig. 4. Distribution of excess pore water pressure at different time.

the closed-form result is slower than PIM. Therefore, average permeability can be only used when permeability varies a little even for one-dimensional consolidation problem. Fig. 6 is an iso-temporal curve for PIM method. All these figures are consistent with Schiffman's results [20].

5.2. Two-dimensional consolidation problem under strip foundation

A two-dimensional consolidation problem is studied here. This is a plane strain consolidation problem under a strip loading. The load is also assumed to be 10 kPa to simulate road load. Foundation soil is

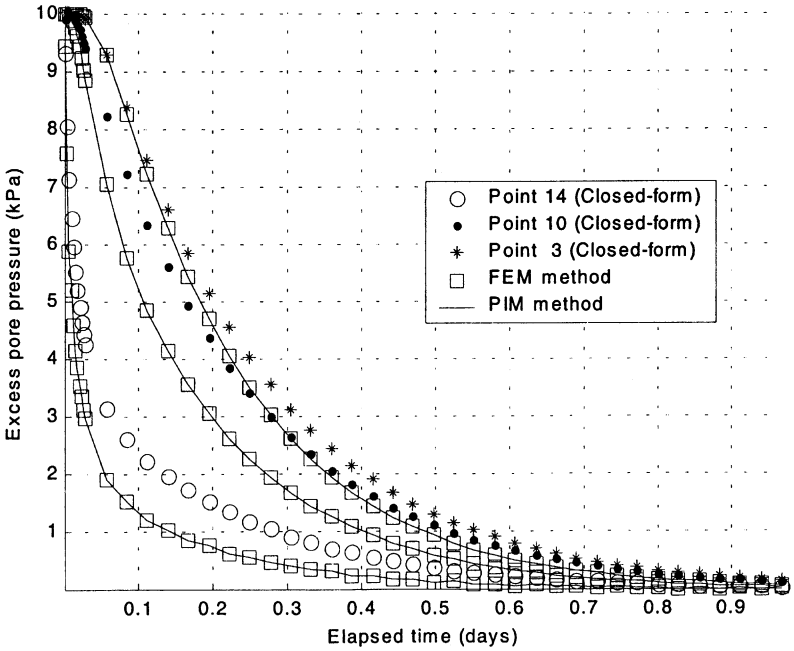

Fig. 5. Distribution of excess pore water pressure for distributive permeability (here closed-form solution based on average permeability).

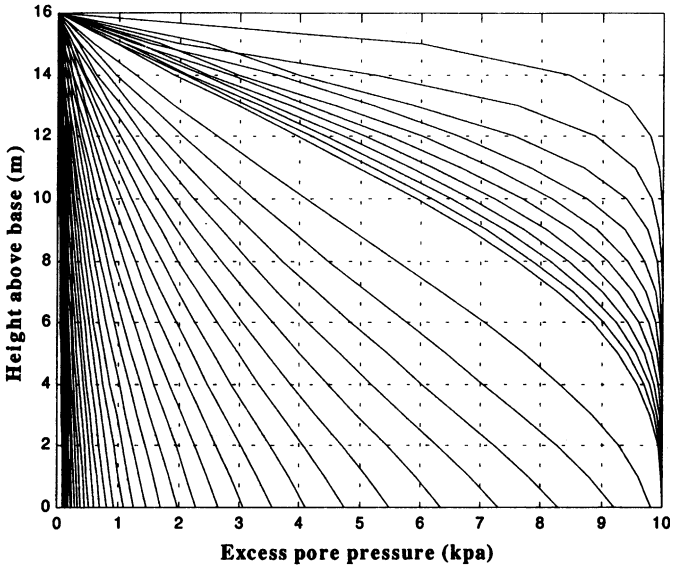

Fig. 6. Iso-temporal distribution of excess pore water pressure (top permeability is 100 times of bottom).

assumed to be linear elasticity, too. A schematic model is shown in Fig. 7. Top surface is fully drainage and the rest boundaries are all impervious. For displacement boundaries, vertical boundaries fix horizontal freedom and the horizontal boundaries fix vertical freedom. There is no closed-form solution, thus FEM is applied for comparison. Fig. 8 shows the settlement distribution at different consolidation time ($T = 0$, 3, 20 days). The foundation will have an immediate settlement after load. Its settlement will increase with the dissipation of excess pore water pressure. The dissipation history of excess pore water pressure at two different points is shown in Fig. 9. When time elapses about 20 days, dissipation of excess pore water

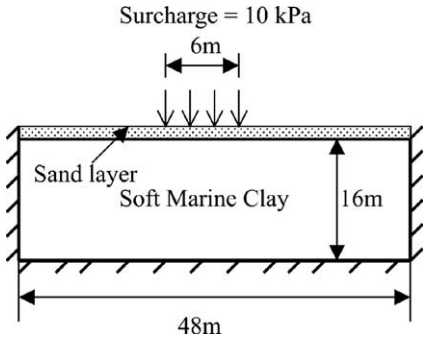

Fig. 7. Two-dimensional consolidation problem under strip load.

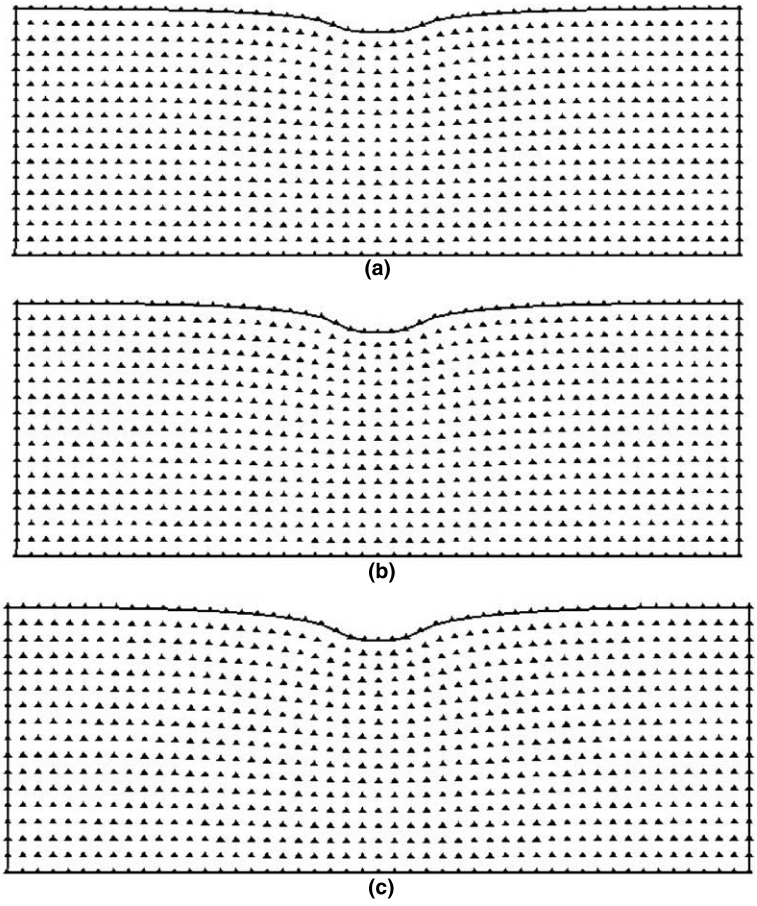

Fig. 8. Settlement distribution at different times: (a) $T = 0$ days; (b) $T = 3$ days; (c) $T = 20$ days.

pressure is almost complete and settlement, u_y, reaches its stable state as shown in Fig. 10. For more details, two sections, a horizontal and a vertical ones, are taken to observe the distributions of excess pore water pressure and effective stress (σ'_y) . The horizontal section is 2 m below from ground level. Along this section, the excess pore water pressure is shown in Fig. 11(a) and the effective stress (σ'_y) is in Fig. 11(b). The excess pore water pressure reaches its peak right below the strip load. It approaches to zero gradually with consolidation. The effective stress increases little immediately after loading. With consolidation, the excess pore water pressure is transferred to soil skeleton. This makes the effective stress to increase gradually. It

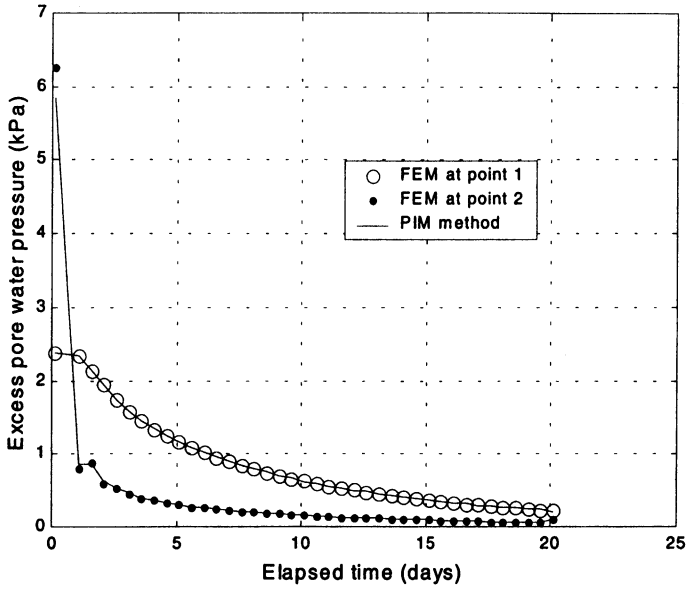

Fig. 9. Excess pore water pressure history at different points.

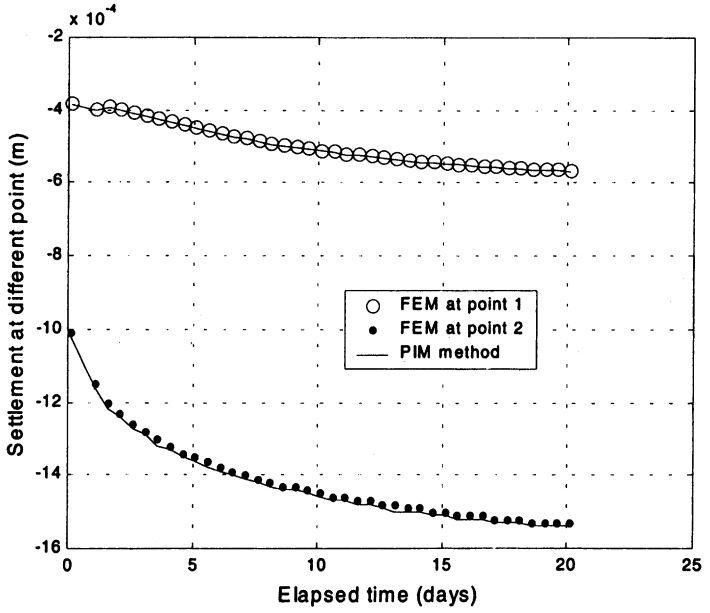

Fig. 10. Settlement history at different points.

reaches its peak at last. The vertical section locates at middle line. Fig. 11(c) shows the dissipation of excess pore water pressure and Fig. 11(d) shows its effective stress (σ'_y) . All these show good agreement with FEM results.

Finally, the effect of irregularity of nodal distribution is studied for this two-dimensional problem. A typical irregular distribution of nodes is given in Fig. 12. The regular distribution of nodes is already given in Fig. 1(b). The nodal density is almost the same. Fig. 13 shows that they have little difference. This difference is biggest at the beginning. Therefore, the irregularity of nodal distribution will affect the accuracy of the PIM method but this effect is within small range.

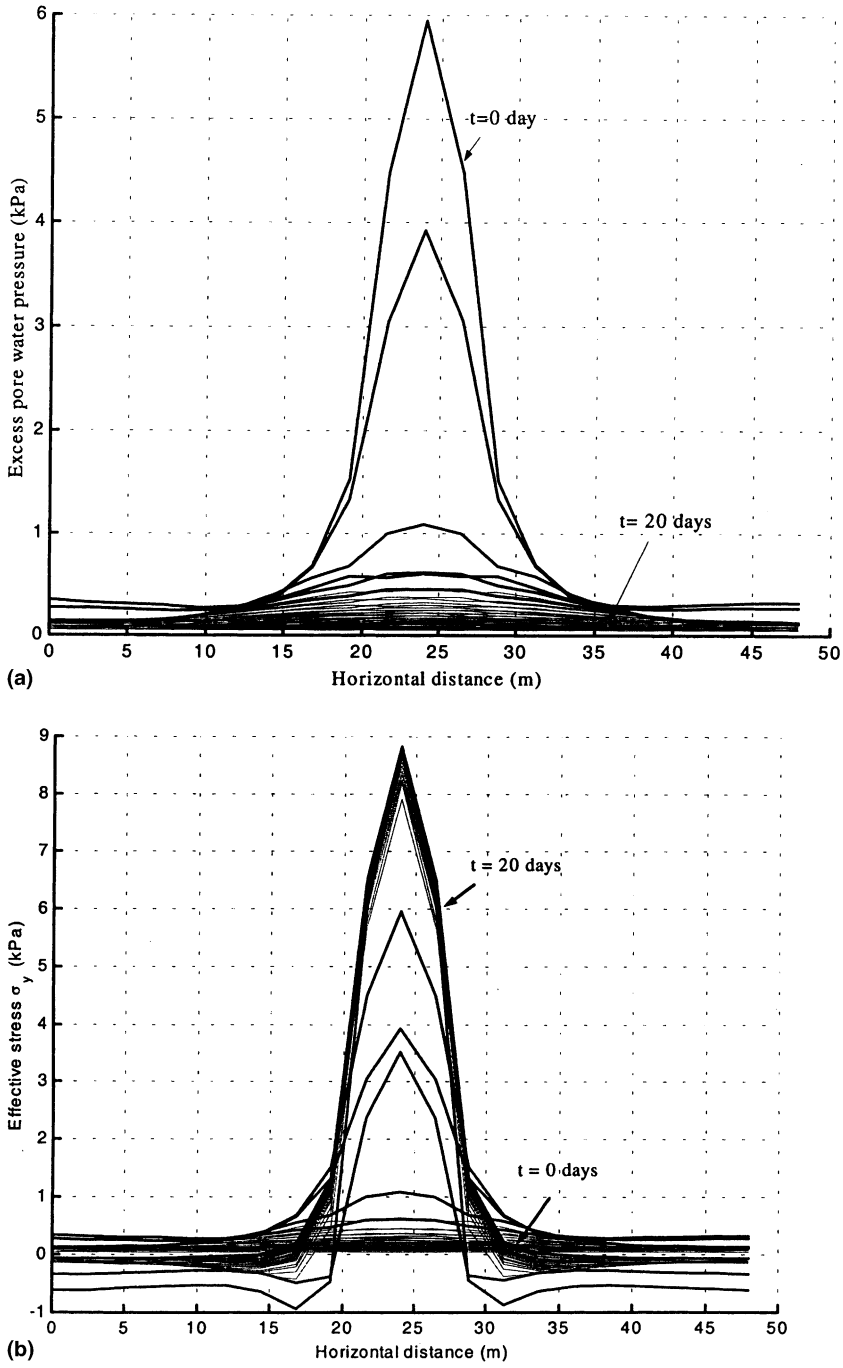

Fig. 11. Stress and excess pore water pressure at different sections: (a) dissipation of excess pore water on surface 2 m below ground; (b) effective stress distribution on surface 2 m below ground; (c) excess pore water along vertical middle line; (d) effective stress σ'_y along vertical middle line.

6. Conclusions

The improved point interpolation meshless method (PIM) is applied to study the numerical solution of Biot's consolidation problem in foundation engineering. We first study the expression of the Biot's theory for general constitutive laws of soil skeleton. A weak form for auto-error corrector is developed based on this expression. Spatial variables of displacement increment and excess pore water pressure are all

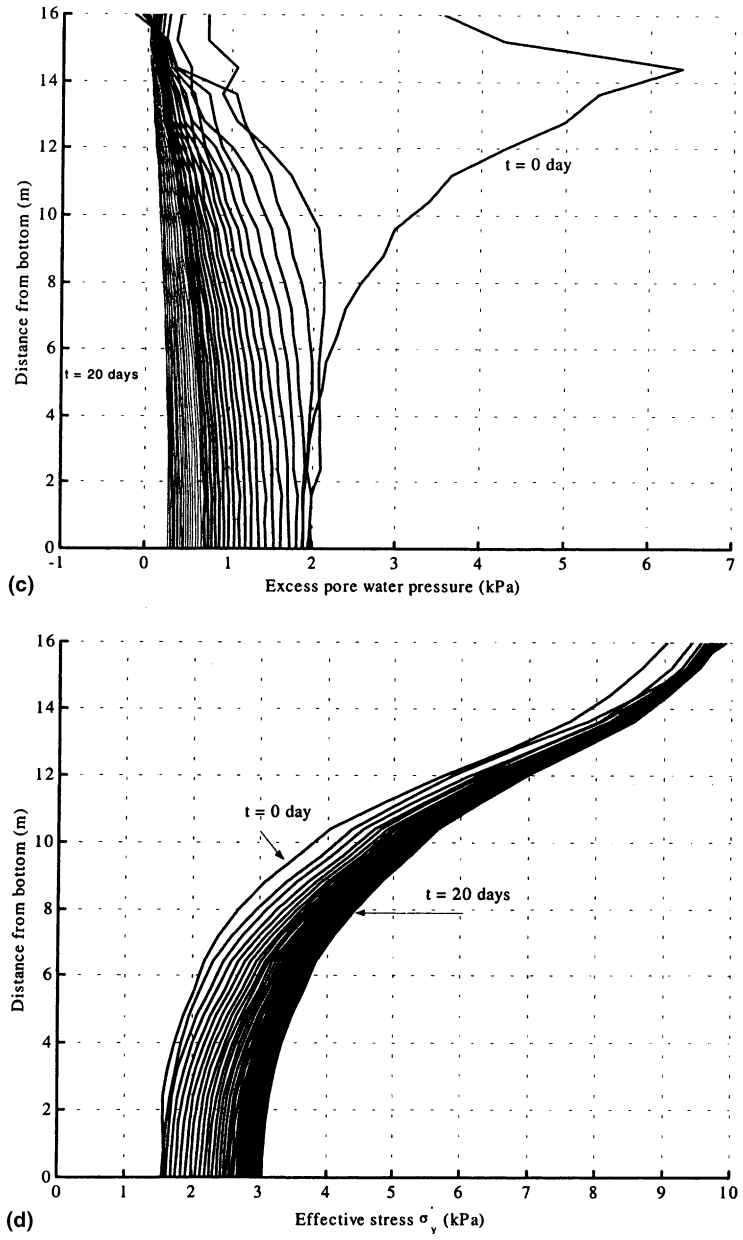

Fig. 11. (Continued).

discretized by the same order of PIM shape function. Time domain is discretized by the Crank–Nicholson method. Some examples demonstrate its feasibility and effectiveness. From these studies, the following conclusions can be drawn:

First, the weak form can automatically correct the error during each time-step and thus keep the same accuracy of global balance. This correction prevents the propagation of numerical error with time-step. On this meaning, the weak form is useful not only for the numerical solution of Biot's consolidation problems but also for nonlinear problems.

Second, improved PIM is an effective method to discretize spatial variables (displacement and excess pore water pressure). Unlike other meshless methods, improved PIM method has simple function and derivatives. Its shape function is of explicit expression and its derivatives are easy to get after $\mathbf{P}_0^{-1}$ is

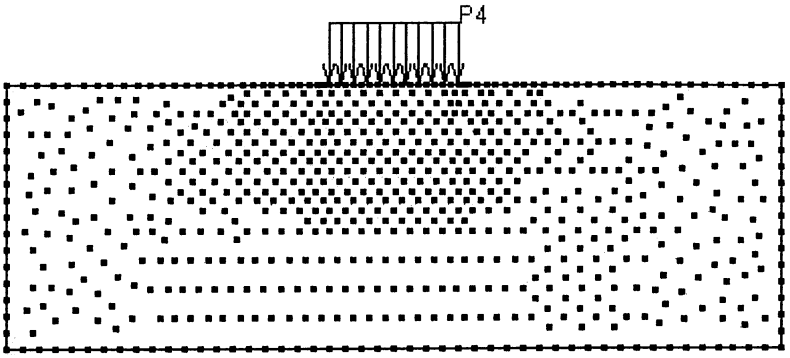

Fig. 12. Irregular distribution of node for two-dimensional problem.

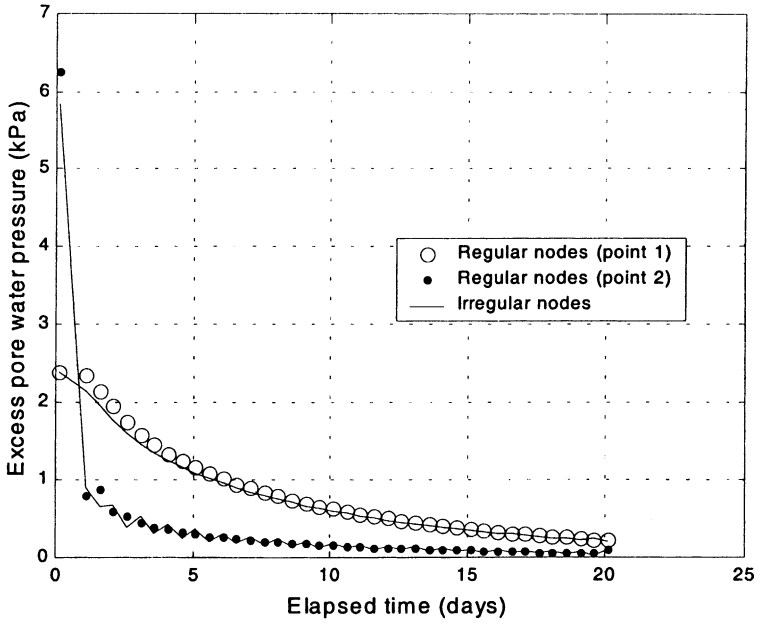

Fig. 13. Effect of irregularity of nodal distribution on excess pore water pressure.

obtained. They are all polynomials. Essential boundary conditions are easily implemented due to the delta function properties of shape function, thus it is of higher computational efficiency.

Third, the same order of shape function for both displacement and excess pore water pressure is feasible to avoid spatial oscillation if time-step is within some range. This range is associated with the minimum distance of nodes and soil parameters like deformation modulus and permeability. The detail on auto-time stepping of PIM method will be given later.

References

[1] B. Nayroles, G. Touzot, P. Villon, Generalizing the finite element method: diffuse approximation and diffuse elements, Comput. Mech. 10 (1992) 307–318.
[2] W.K. Liu, S. Jun, Y.F. Zhang, Reproducing kernel particle methods, Int. J. Numer. Methods Fluids 20 (1995) 1081–1106.
[3] C.A. Duarte, J.T. Oden, Hp clouds – an h–p meshless method, Numer. Methods Partial Differential Equations 12 (1996) 673–705.
[4] E. Onate, S. Idelsohn, O.C. Zienkiewicz, R.L. Taylor, A finite point method in computational mechanics – applications to convective transport and fluid flow, Int. J. Numer. Methods Engrg. 39 (1996) 3839–3866.
[5] T. Belytschko, Y.Y. Lu, L. Gu, Element-free Galerkin methods, Int. J. Numer. Methods Engrg. 37 (1994) 229–256.

[6] T. Belytschko, Y. Krongauz, D. Organ, M. Fleming, P. Krysl, Meshless methods: an overview and recent development, Comput. Methods Appl. Mech. Engrg. 139 (1996) 3–47.
[7] Y.Y. Lu, T. Belytschko, L. Gu, A new implementation of the element-free Galerkin method, Comput. Methods Appl. Mech. Engrg. 113 (1994) 397–414.
[8] H. Modaressi, P. Aubert, Element-free Galerkin method for deforming multiphase porous media, Int. J. Numer. Methods Engrg. 42 (1998) 313–340.
[9] P. Lancaster, K. Salkauskas, Surfaces generated by moving least-squares methods, Math. Comput. 37 (1981) 141–158.
[10] T. Zhu, S.N. Atluri, A modified collocation method and a penalty formulation for enforcing the essential boundary conditions in the element free Galerkin method, Comput. Mech. 21 (1998) 211–222.
[11] G.J. Wagner, W.K. Liu, Application of essential boundary conditions in mesh-free methods: a corrected collocation method, Int. J. Numer. Methods Engrg. 47 (8) (2000) 1367–1379.
[12] Y.X. Mukherjee, S. Mukherjee, The boundary node method for potential problems, Int. J. Numer. Methods Engrg. 40 (5) (1997) 797–815.
[13] P. Breitkopf, A. Rassineux, G. Touzot, P. Villon, Explicit form and efficient computation of MLS shape functions and their derivatives, Int. J. Numer. Methods Engrg. 48 (3) (2000) 451–466.
[14] K.T. Danielson, S. Hao, W.K. Liu, R. Aziz Uras, S. Li, Parallel computation of meshless methods for explicit dynamic analysis, Int. J. Numer. Methods Engrg. 47 (7) (2000) 1323–1341.
[15] G.R. Liu, Y.T. Gu, A point interpolation method for two-dimensional solids, Int. J. Numer. Methods Engrg. 50 (2001) 937–951.
[16] J.G. Wang, G.R. Liu, Radial point interpolation method for elastoplastic problems, in: Proc. of the 1st Int. Conf. on Structural Stability and Dynamics, Taipei, 7–9 December 2000, pp. 703–708.
[17] M.A. Biot, General theory of three-dimensional consolidation, J. Appl. Phys. 12 (1941) 155.
[18] P. Lancaster, K. Salkauskas, Curve and Surface Fitting. An Introduction, Academic Press, New York, 1986.
[19] K. Terzaghi, R.B. Peck, Soil Mechanics in Engineering Practice, 2nd ed., Wiley, New York, 1976.
[20] R.L. Schiffman, R.E. Gibson, Consolidation of non-homogeneous clay layers, in: Proceedings of ASCE, JSMFD, 90(SM5), 1964.